Zeitschrift für Physikalische Chemie, Bd. 201, S. 31–43 (1997)

Behaviour of the V^{2+} Ground State in Tetrahedrally Coordinated II–VI Semiconductors*

By S. W. Biernacki[1], J. Kreissl[2] and H.-J. Schulz[3]

[1] Institute of Physics, Polish Academy of Sciences, Al. Lotników 32/46, PL-02668 Warsaw, Poland
[2] Arbeitsgruppe EPR am Institut für Festkörperphysik, Technische Universität Berlin, Rudower Chaussee 5, D-12484 Berlin, Germany
[3] Fritz-Haber-Institut der Max-Planck-Gesellschaft, Faradayweg 4–6, D-14195 Berlin, Germany

(Received August 25, 1996; accepted September 23, 1996)

Electron paramagnetic resonance / Jahn-Teller effect / Photo-luminescence / Tanabe-Sugano calculation / Tunnelling splitting

The ground state of the lattice-neutral charge state of vanadium in tetrahedrally coordinated II–VI materials is a $^4T_1$ term and is hence subject to a Jahn-Teller (JT) effect. In this paper photo-luminescence and EPR investigations on V^{2+} ($3d^3$) in ZnS, ZnSe, ZnTe, and CdTe are combined with Tanabe-Sugano calculations including JT interaction. For ZnS the no-phonon structure is explained by a tunnelling splitting.

1. Introduction

Applications of the photorefractive effect in the infrared region, where fibre optics communication is operated, are based on II–VI semiconducting materials. For the photorefractive behaviour of these materials, V-related defects play an outstanding role among the transition metals. This fact has renewed the interest in information on the nature of V centres. Transition metal ions commonly substitute for cations, thus implying the general possibility of amphoteric changes between their charge states. Starting from the lattice-neutral state (2+), donor-type (2+/3+) as well as acceptor-type (2+/+) conversions are conceivable. For a long time, the knowledge about the lattice-neutral V^{2+} ($3d^3$) charge state was by no means comprehensive. Only in the last years the verification of the presence of V^{2+} by lumi-

* Presented at the 13th International Symposium on Electrons and Vibrations in Solids and Finite Systems (Jahn-Teller Effect) Berlin 1996.

Table 1. The interatomic distances in Å: d_i – the sum of ionic radii, d_c – the sum of covalent radii, d_{cal} – the bondlength calculated from bond energy.

	ZnS	ZnSe	ZnTe	CdTe
d_{exp}	2.341	2.455	2.642	2.805
d_i	0.74+1.84=2.58	0.74+1.91=2.65	0.74+2.11=2.85	0.97+2.11=3.08
d_c	1.25+1.02=2.27	1.25+1.16=2.41	1.25+1.36=2.61	1.48+1.36=2.84
$d_i(V^{2+}\text{-anion}^{2-})$	0.88+1.84=2.79	0.88+1.91=2.79	0.88+2.11=2.99	0.88+2.11=2.99
$d_c(V^0\text{-anion}^0)$	1.22+1.02=2.24	1.22+1.16=2.38	1.22+1.36=2.58	1.22+1.36=2.58
d_{cal}(V-anion)	2.36	2.48	2.75	2.75

nescence and electron paramagnetic resonance (EPR) studies has been successful in ZnS, ZnSe, CdTe, and ZnTe [1–8]. In this communication, fine-structure peculiarities in the emission spectra will be discussed in the light of the observed different JT coupling mechanisms as analysed by EPR. The derived level schemes of the ground-state splitting will be presented and combined with more fundamental Tanabe-Sugano calculations.

2. V^{2+}-anion bondlength

The V^{2+} ion enters a II–VI lattice substitutionally on a cation lattice site. The II–VI compounds have various interatomic distances d_{exp} as listed in row 2 of Table 1. It will be interesting to find out how the substitutional V atom matches the interatomic distance of the host crystal. To this end, we first consider how accurately the interatomic distance can be represented as a sum of the corresponding radii in an undisturbed crystal. In row 3 the distance d_i is shown as a sum of the ionic radii which represent the effective size of a charged atom in an ionic compound. The first item in this sum is the cation radius in the charge state 2+, while the second is the anion radius (charge state −2). It is seen that d_i exceeds d_{exp} by up to 10%. In row 4 the results of the opposite approximation are presented. The distance d_c is now taken as the sum of the covalent radii which represent the effective size of an atom in a covalent bond. In this case the distance d_c is smaller than d_{exp} (except for CdTe) and matches d_{exp} with an accuracy of 3%.

Similar results are given in rows 5 and 6, supposing the V atom replaces the cation of the host crystal. Again the sum of the covalent radii matches d_{exp} better and it is seen that in all cases a breathing mode distortion around the defect should be expected. Finally, in the last row we give the bondlength calculated from the bond energies. The latter were computed using the corresponding expression given by Harrison [9]. In this bond energy calculation we used the following one-electron atomic energies for the V atom: $\varepsilon_{4s} = -6.3$ eV and $\varepsilon_{4p} = -3.3$ eV. The latter value follows from a very rough interpolation, in which the additional condition was used that

d_{cal} should match approximately d_{exp} for ZnS. Then for the other crystals d_{cal} fits d_{exp} fairly well. From this consideration follows that there is no dramatic symmetric or asymmetric distortion around the V atom when it enters a cation lattice site substitutionally. Consequently, one should not expect a large static low-symmetry crystal field around the V atom.

3. Jahn-Teller coupling

If a transition metal defect has an orbital degeneracy in the ground state, the system is unstable towards asymmetric displacements of the neighbouring atoms. For a defect with a T_1 electronic ground state in a crystal field of tetrahedral symmetry, like the V^{2+} ion, the possible asymmetric distortions can have t_2 (trigonal), e (tetragonal) or ($t_2 + e$) orthorhombic symmetry. Estimations of the JT coupling constants based on a point charge model show that the trigonal distortion is dominating. For V^{2+} in ZnS this evaluation has been confirmed by EPR [5]. These distortions and their effects on the electronic states can be represented as

$$V = V_D (Q_\theta E_\theta + Q_\varepsilon E_\varepsilon) + V_T (Q_\xi T_\xi + Q_\eta T_\eta + Q_\zeta T_\zeta) \quad (1)$$

where V_D and V_T are the coupling coefficients for the tetragonal and trigonal distortions, respectively. Q_θ, Q_ε, Q_ξ etc. are the normal coordinates and E_θ, E_ε, T_ξ etc. are electronic operators in the given electronic state [10]. The atoms in a crystal vibrate thermally around this equilibrium position. The amplitude of this harmonic vibration is approximately 2% of the equilibrium interatomic distance. If under an asymmetric distortion the ligand is displaced from the lattice site by a value smaller than the amplitude of the harmonic vibration, the Jahn-Teller coupling is weak. In this situation the four geometrically equivalent positions of the trigonal distortion interact strongly. As a result of this interaction, the fourfold geometrical degeneracy is reduced into a vibronic triplet and a singlet. The ground state is the vibronic triplet while the vibronic singlet lies higher. The energy difference between this singlet and the lower vibronic triplet is the tunnelling splitting energy [11, 12]. In case of a very strong asymmetrical distortion of ligands (as compared with the amplitude of the harmonic vibrations), the four geometrical positions of a trigonal distortion can be considered as nearly noninteracting. This is the example of a strong Jahn-Teller coupling with accidental fourfold degeneracy. It is not possible to estimate the coupling constant V_T in (1) reliably by theoretical methods. Presumably, in II–VI compounds a coupling of intermediate strength takes place. Therefore we shall try to extract as much information as possible from the experimental spectra using the known theoretical framework.

Before determining the peculiarities of the JT interaction, we should find parameters which describe the crystal-field levels. To this end we cal-

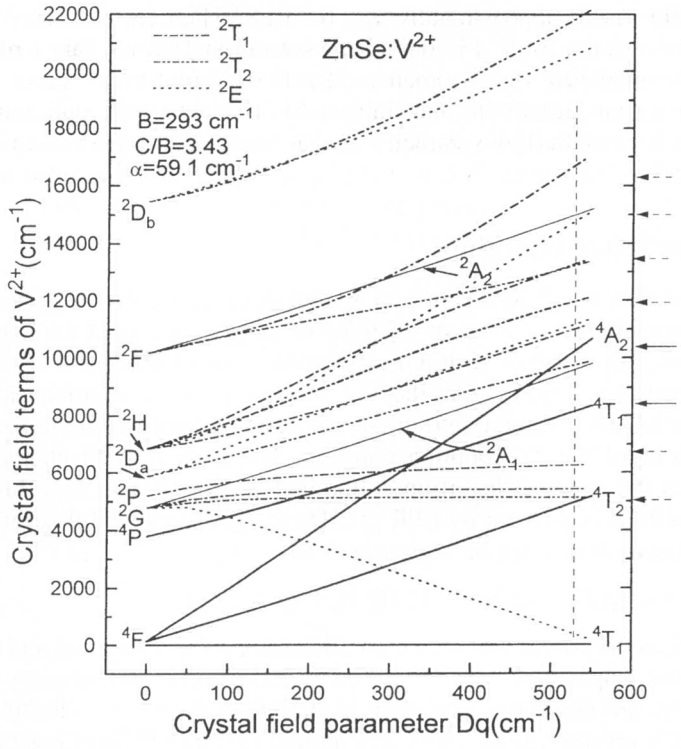

Fig. 1. Tanabe-Sugano fit for the V^{2+} ($3d^3$) ion in ZnSe. The solid arrows on the right denote those experimental data used in the fit while dashed arrows indicate additional experimental data.

culated the Tanabe-Sugano matrices and some of the term energies were fitted to the known experimental transitions. In our calculations, the Tanabe-Sugano matrices included the tetrahedral crystal-field splitting parameter Dq, the parameter α of the Trees correction [13] and the Racah parameters B and C. The value of α was adopted from the terms of the free V^{2+} ion. It turned out that this parameter improves the free-ion energies essentially and is therefore sustained in the description of the crystal levels which arise from the free-ion terms. Moreover, in the calculation of the crystal levels we keep the ratio C/B the same as for the free ion. Hence, our Tanabe-Sugano matrices contain only two adjustable parameters: Dq and B. Fig. 1 shows the Tanabe-Sugano diagram for V^{2+} in ZnSe. The solid arrows on the right in Fig. 1 denote those experimental data used in the fit while dashed arrows indicate additional experimental data.

Now we proceed towards the determination of the JT energy for a trigonal distortion in the $^4T_1(F)$ ground level. To this end we shall only use the

information available on the splitting of the $^4T_1(P)$ term, known from the excitation spectra. This splitting is equal to $3\,E_{JT}(^4P)$ and takes place for some unknown distortion coordinate Q. This distortion is caused by the interaction Hamiltonian (1). We calculated Eq. (1) by an expansion of the crystal field into series for the trigonal and tetragonal distortions. Only the second-order harmonics in the crystal potential were taken into account. The energy matrices including the trigonal distortions for the T_1 and T_2 levels of the V^{2+} ion have the following form:

	$T_{1\zeta}(^4P)$	$T_{1\gamma}(^4P)$	$T_{1\varepsilon}(^4P)$	$T_{1\gamma}(^4F)$	$T_{1\gamma}(^4F)$	$T_{1\varepsilon}(^4F)$
$T_{1\gamma}(^4P)$	$-8\,Dq-12\,B+10\,\alpha$	$V_T\,Q_\zeta/2$	$V_T\,Q_\eta/2$	$-6\,B+4\,\alpha$	$-V_T\,Q_\zeta$	$-V_T\,Q_\eta$
$T_{1\gamma}(^4P)$	$V_T\,Q_\zeta/2$	$-8\,Dq-12\,B+10\,\alpha$	$V_T\,Q_\xi/2$	$-V_T\,Q_\zeta$	$-6\,B+4\,\alpha$	$-V_T\,Q_\xi$
$T_{1\varepsilon}(^4P)$	$V_T\,Q_\eta/2$	$V_T\,Q_\xi/2$	$-8\,Dq-12\,B+10\,\alpha$	$-V_T\,Q_\eta$	$-V_T\,Q_\xi$	$-6\,B+4\,\alpha$
$T_{1\gamma}(^4F)$	$-6\,B+4\,\alpha$	$-V_T\,Q_\zeta$	$-V_T\,Q_\eta$	$-8\,Dq-2\,B+10\,\alpha$	$V_T\,Q_\zeta$	$V_T\,Q_\eta$
$T_{1\gamma}(^4F)$	$-V_T\,Q_\zeta$	$-6\,B+4\,\alpha$	$-V_T\,Q_\xi$	$V_T\,Q_\zeta$	$-8\,Dq-12\,B+10\,\alpha$	$V_T\,Q_\xi$
$T_{1\varepsilon}(^4F)$	$-V_T\,Q_\eta$	$-V_T\,Q_\xi$	$-6\,B+4\,\alpha$	$V_T\,Q_\eta$	$V_T\,Q_\xi$	$-8\,Dq-12\,B+10\,\alpha$

	$T_{2\xi}(^4F)$	$T_{2\eta}(^4F)$	$T_{2\zeta}(^4F)$
$T_{2\xi}(^4F)$	$2\,Dq-15\,B+12\,\alpha$	$V_T\,Q_\zeta/2$	$V_T\,Q_\eta/2$
$T_{2\eta}(^4F)$	$V_T\,Q_\zeta/2$	$2\,Dq-15\,B+12\,\alpha$	$V_T\,Q_\xi/2$
$T_{2\zeta}(^4F)$	$V_T\,Q_\eta/2$	$V_T\,Q_\xi/2$	$2\,Dq-15\,B+12\,\alpha$

Now, if we take a particular value of the unknown distortion coordinate (e.g. $Q=1$), we obtain the dependence of the spin-quartet terms on V_T. First, we realize that the trigonal splitting is nearly comparable for the levels $^4T_2(F)$ and $^4T_1(F)$. This indicates that the no-phonon lines (NPL) of the transition between these levels correspond approximately to the energy of the cubic-field splitting parameter, because the trigonal configuration minima for the $^4T_2(F)$ term lie at only slightly smaller coordinates than for the $^4T_1(F)$ term. This observation is supported by the strength of the NPL for V^{2+} in ZnS (Fig. 2a) which is large enough to imply a small Huang-Rhys factor (note that it also depends on the frequency of the coupling mode). In the case of ZnSe (Fig. 2b) there are three NPL because the whole emission spectrum is a superposition of at least three shifted spectra (see discussion below). Their individual height is smaller than in ZnS but they are still pronounced. The emission spectrum also contains a transition to a doublet which is by an energy $3\,E_{JT}$ higher than the ground singlet (broad band, left of the NPL). A second observation is that the splitting of the $^4T_1(P)$ term

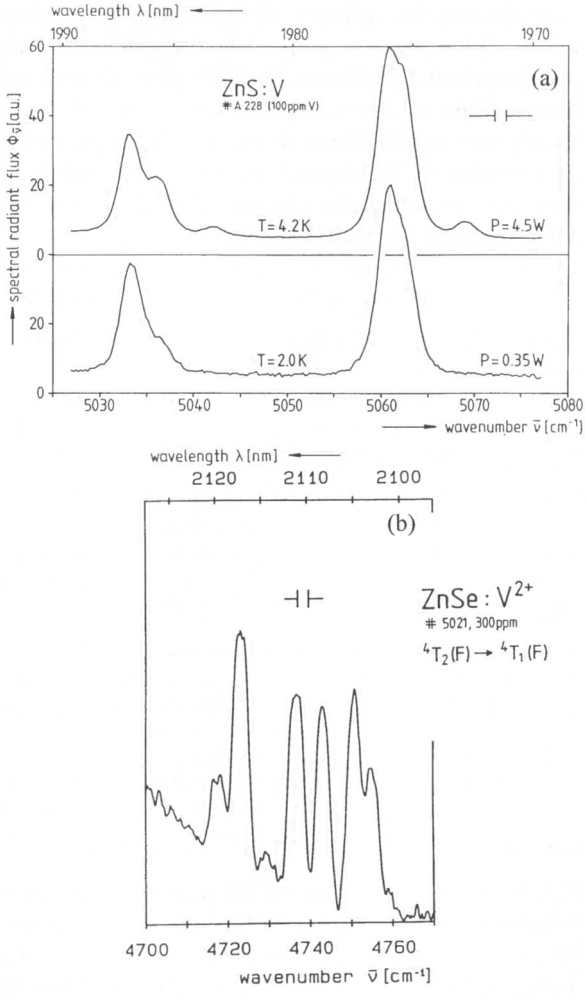

Fig. 2. NPL's of the V^{2+} ion in (a) ZnS [1] and (b) ZnSe [2].

under a trigonal distortion is nearly 1.5 times larger than the splitting of $^4T_1(F)$. This effect arises from coupling between these terms, i.e. from off-diagonal terms containing V_T. Consequently, the configuration minima for the upper term are at a higher Q than those for the ground state. If we denote by a the trigonal splitting of the $^4T_1(F)$ term (for arbitrary V_T) and by b the similar splitting for the term $^4T_1(P)$, we have the relation $E_{JT}(^4F) = aE_{JT}(^4P)/b$. We found the ratio $a/b \approx 2/3$, independent of the particular values of Q and V_T or the elastic energy. The elastic energy enters the diagonal elements of the interaction matrices, and it is the same for all

terms. $E_{JT}(^4P)$ is equal to 1/3 of the splitting of the $^4T_1(P)$ term and can be read directly from the excitation spectra. However, from the excitation spectra for V^{2+} only the JT splitting of $T_1(^4P)$ at the trigonal distortion minimum for the ground state can be determined (assuming that the transition obeys the Franck-Condon principle). For example, in ZnS $E_{JT}(^4P) = 825/3\ cm^{-1}$, therefore $E_{JT}(^4F) \approx 180\ cm^{-1}$. In ZnSe $E_{JT}(^4P) = 420/3\ cm^{-1}$, so that $E_{JT}(^4F) \approx 95\ cm^{-1}$.

Now, the question arises how strong is the electron-lattice coupling. Usually, the strength of the coupling is expressed in terms of the ratio $\gamma = E_{JT}(^4F)/\hbar\omega$, where ω marks an average frequency of the ligand vibrations. Sometimes, ω is taken to be the transversal acoustic frequency of the crystal at the points X and L, i.e. 90 to 70 cm^{-1} for ZnS and 70 to 60 cm^{-1} for ZnSe. In this case, the coupling for the V^{2+} ion in ZnS should be considered as nearly strong, and as intermediate for ZnSe. This estimation is considered as extreme since these transversal frequencies correspond to a bending of the TM-ligand bond. In reality, the trigonal distortion includes extension and contraction of the bond as well, i.e. stretching frequencies. Hence, for an assessment of the coupling it is preferable to derive some average frequency from the complete phonon spectrum, which can be taken approximately as 2/3 of the optical frequency at the Γ point. For ZnS this gives rise to an average of $\omega \approx 200-220\ cm^{-1}$, while for ZnSe $\omega \approx 150-170\ cm^{-1}$. Under these assumptions, the coupling is rather intermediate in both cases (much closer to the limit of the weak regime than to the strong coupling domain).

4. Fine structure in EPR and emission spectra

The EPR of the V^{2+} ion in ZnS [5] reveals a trigonal symmetry of the ground state. The zero-field splitting, estimated to about 4 cm^{-1}, was attributed to spin-orbit interaction. We check the validity of this finding by calculating the spin-orbit splitting of the $^4T_1(F)$ level for various values of the trigonal distortion, assuming a spin-orbit constant $\lambda \approx 30\ cm^{-1}$. The reduction compared with the free-ion value 59 cm^{-1} is caused by the JT orbital reduction factor [10] and the covalency effect. The lowest level corresponds to a Γ_8 representation and is split into two sublevels separated by $\approx 4\ cm^{-1}$. In the emission, Γ_8 is seen as one slightly boradened line. On the other hand, the NPL of the $ZnS:V^{2+}$ emission exhibit a $\approx 28\ cm^{-1}$ splitting which cannot be attributed to this spin-orbit interaction. We assign this finding to the tunnelling splitting E_{TU} between the four equivalent minima related to the trigonal distortion [11, 12]. In fact, such a splitting takes place for the whole range of JT coupling (with the only exception of a very strong JT interaction). The effect is caused by an overlap of the oscillator potential wells located at the particular minima. The derived energy scheme

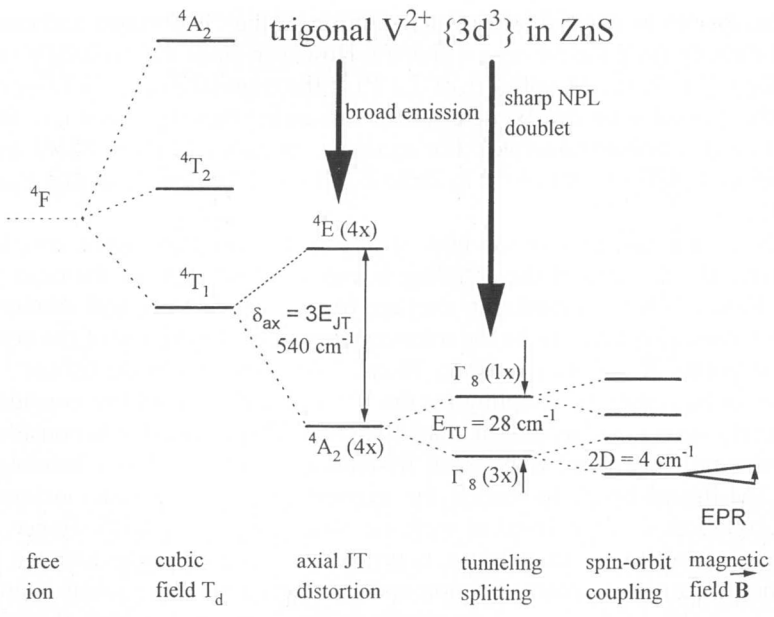

Fig. 3. Schematic splitting of the $^4T_1(F)$ ground state of the V^{2+} impurity ion in ZnS. In brackets the geometrical degeneracy is denoted.

for the lowest levels of the V^{2+} ion in ZnS is depicted in Fig. 3. The emission NPL correspond to transitions from the $^4T_2(F)$ crystal-field level to the lowest Γ_8 levels. The broad emission band originates from the transition from $^4T_2(F)$ to the lowest ^4E level (which can be also broadened, owing to tunnelling splitting and a possible additional tetragonal distortion).

It is known that infrared vibrational spectra exhibit a fine structure as a result of isotopic effects. For instance, the local-mode line of Si_{As} in GaAs was resolved into a doublet [14] with a separation of 1.15 cm^{-1}. This splitting was attributed to the occurrence of the two nuclides ^{69}Ga and ^{71}Ga as nearest neighbours of Si_{As}. Although the effect is small (≈ 1 cm^{-1}), it indicates that small asymmetrical distortions caused by a random distribution of various isotopes take place. However, if the electronic state is JT active, the isotope distribution around a defect can initialize certain types of additional, e.g. tetragonal distortions. Under these conditions an electronic distortion energy can be remarkably larger (because it depends on the particular JT coupling coefficient) and the occurrence of the distortion is proportional to the number of configurations of the type from which it arises. As seen from Table 2, isotopic distribution effects should be absent for V^{2+} in ZnS because there is practically only one sulfur isotope, which has an abundance of 95.0%. From the point of view of isotopic abundance such an

Table 2. Stable isotopes of V and its nearest neighbours – S, Se and Te.

Isotope	Weight	Abund., %	Isotope	Weight	Abund., %
^{50}V	49.9472	0.25	^{32}S	31.9721	95.0
^{51}V	50.9440	99.77	^{33}S	32.9715	0.76
^{120}Te	119.9040	0.089	^{34}S	33.9679	4.22
^{122}Te	121.9031	2.46	^{36}S	35.9671	0.02
^{123}Te	122.9043	0.87	^{74}Se	73.9225	0.9
^{124}Te	123.9028	4.61	^{76}Se	75.9192	9.0
^{125}Te	124.9044	6.99	^{77}Se	76.9199	7.6
^{126}Te	125.9033	18.71	^{78}Se	77.9173	23.5
^{128}Te	127.9045	31.79	^{80}Se	79.9165	49.8
^{130}Te	129.9063	34.48	^{82}Se	81.9167	9.2

effect might be expectable also in ZnTe and CdTe (see Table 2). The local-mode splitting should be smaller for the Te than for Se isotopes because of the smaller deviation of the mass. If the main trigonal distortion is weaker, the additional distortion initialized by the isotope substitution can become stronger. Further possible implications of the isotopic distribution effect will be discussed in the next section.

5. Discussion

The various interactions between the V impurity and its nearest neighbours manifest themselves in different experiments. For example, the excitation spectra indicate the amplitude of the main JT distortion (in our case the splitting of the $^4T_1(P)$ level), the emission spectra provide the energy of the lowest transition between the crystal-field components and, in addition, signs of a fine structure due to spin-orbit as well as JT couplings. EPR results reveal the local symmetry around a defect as well as the spectroscopic splitting factors. Using the described theoretical model we shall present a picture which arises from these various sources of information. EPR spectra are conveniently described using a spin Hamiltonian. The spectroscopic factor is determined from analysis of the observed resonance spectra. On the other hand, it is expressed in terms of the matrix elements of the orbital momentum between electronic states and in terms of energy distances between these states. These matrix elements are reduced owing to an admixture of ligand wave functions to those of the defect (covalency) as well as owing to a replacement of the electronic wave function by vibronic functions (electron-lattice coupling). It is very difficult to account quantitatively for both effects, and this implies that information of the energy differences (for example, the JT energy) extracted from the knowledge of the g

factor is not accurate enough. Therefore, the optical spectra were used here to obtain information on the energy distances. We shall now discuss details of the spectra for particular crystals.

V^{2+} in ZnS

EPR measurements suggest a trigonal distortion. Some information on the energy of this distortion can be obtained from the excitation band $^4T_1(F) \rightarrow {}^4T_1(P)$ which is split (note that the configuration minima in the initial and final states are at different coordinates Q). We estimate the energy $E_{JT}(^4F)$ of the trigonal distortion in the $^4T_1(F)$ level as 180 cm^{-1}. The isotopic effect is absent, as there is only one S nuclide (^{32}S) with dominating abundance. The NPL in the $^4T_2(F) \rightarrow {}^4T_1(F)$ emission shows a 28 cm^{-1} tunnelling splitting E_{TU} (Fig. 2a). The NPL has a first replica shifted towards lower energy by 125 cm^{-1} and, perhaps a second satellite in a distance of 280 cm^{-1}. These energies are assigned to local modes of V^{2+}. Two local modes arise when the host-crystal cation is lighter than the anion. Then a replacement of the cation produces local modes, one near or above the optical and another one near or above the acoustical phonons. A similar effect was observed for Co^{2+} in CdSe [15] where the corresponding local modes were measured as 138.5 and 226.4 cm^{-1}.

V^{2+} in ZnSe

In this case the excitation spectra are similar to ZnS, however, the trigonal distortion of the $^4T_1(P)$ level is smaller. We estimate $E_{JT}(^4F)$ as 95 cm^{-1}. The NPL shows 4 to 5 cm^{-1} spin-orbit splitting and has two replicas, shifted by 12 and 32 cm^{-1} towards smaller energies (Fig. 2b) [2]. Furthermore, this complicated structure has weaker replicas which involve low-energy shifts corresponding to the lattice phonons TA(X) = 70, LA(L) $\approx$ 160, and LO(Γ) $\approx$ 255 cm^{-1}. The spin-orbit splitting $\approx$4 to 5 cm^{-1} is comparable with that in ZnS. The twofold shift of the phonon doublet by 12 and 32 cm^{-1} is attributed to a distribution of Se isotopes. We remind that the differences in the isotope masses do not cause such a large energy shift. They only initialize a possible additional distortion. An inspection of Table 2 indicates that out of the four neighbours of V^{2+} two will be most likely ^{80}Se. Then two other sites can be occupied either by ^{78}Se and ^{80}Se or by two ^{78}Se anions (resulting in a trigonal or orthorhombic distortion) or by ^{78}Se and one of the nuclei ^{76}Se, ^{77}Se, ^{82}Se (triclinic distortion). Therefore, the main trigonal distortion (e.g. bond stretching) can contain an admixture with another trigonal distortion (e.g. bond bending) oriented in a different direction, or an admixture of a tetragonal distortion. In such a case the adiabatic surface of the main trigonal distortion does not possess axial symmetry and

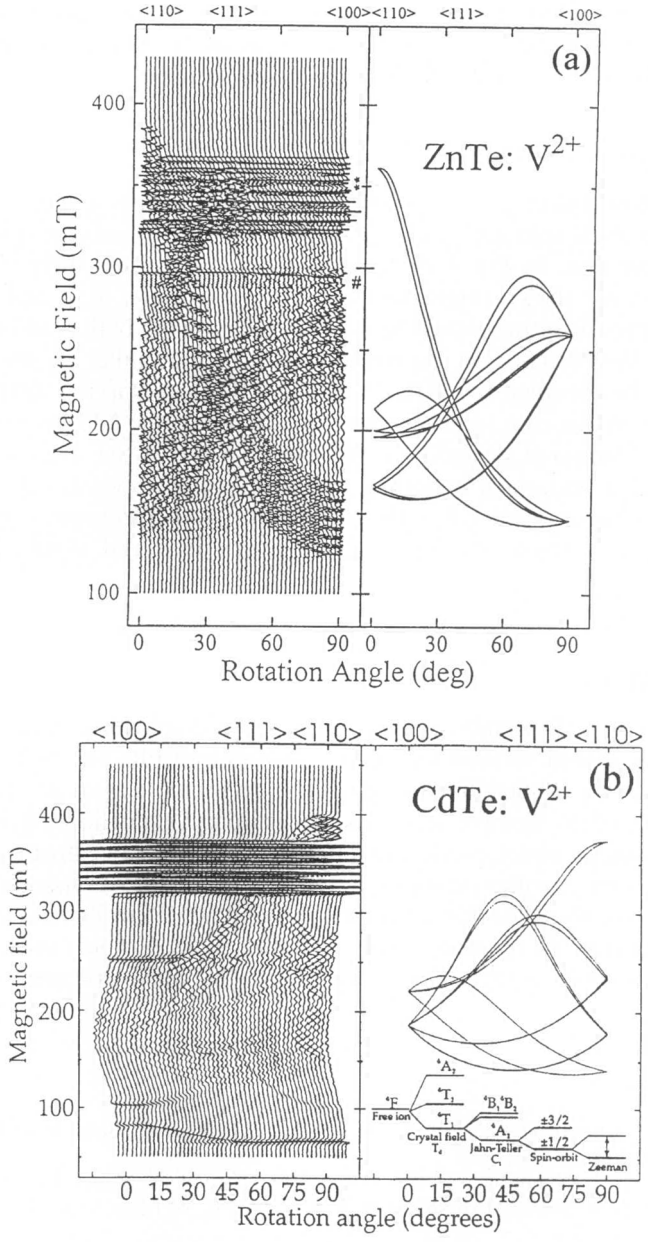

Fig. 4. Experimental (left) and calculated (right) angular dependencies of the triclinic V^{2+} EPR spectra for (a) ZnTe [6] and (b) CdTe [8].

various geometrical combinations of this surface lead to different energy states (here shifted by 12 and 32 cm^{-1}). It might be that the occurrence of this family of V^{2+} centres prevents an EPR detection.

V^{2+} in ZnTe and CdTe

In these host materials the excitation spectra show only a broadening (no clearly resolved splitting). EPR measurements clearly indicate a low-symmetry behaviour. In Fig. 4 the angular dependences and their theoretical description are shown (more details are given in Refs. [6, 7 and 8]). The origin of this distortion should be a JT effect involving both t_2 and e vibronic modes. Furthermore, an inspection of Table 2 shows that the sites nearest to V can be occupied by ^{128}Te, ^{130}Te and ^{126}Te with varying distributions. Therefore, in this case some structure is expected in the NPL as well. However, in comparison to ZnSe the relative changes of the mass are nearly twice smaller and, most important, the JT coupling is weaker. From excitation spectra we read $3\,E_{JT}(^4P) \approx 300\,cm^{-1}$ and this implies $E_{JT}(^4F) \approx 65\,cm^{-1}$. As a result, the NPL cannot be resolved and should be fairly broad.

6. Summary

Estimations of JT coupling constants suggest a dominating trigonal distortion that is indeed verified for the V^{2+} in ZnS by EPR. The NPL structure is explained by a tunnelling splitting. For ZnSe, replicas of the NPL have been assigned to isotopic shifts due to various Se nuclides. It is argued that this isotope effect, producing a number of different centres concerning symmetry and coupling strength, is the reason for the absence of an EPR spectrum in ZnSe. The lower symmetry found at V^{2+} in ZnTe and CdTe is originating from JT coupling involving both t_2 and e vibronic modes. In this case the possible isotope effect may lead to the weak-structured emission spectrum.

References

1. S. W. Biernacki, G. Roussos and H.-J. Schulz, J. Phys. C: Solid State Physics **21** (1988) 5615.
2. G. Goetz, U. W. Pohl and H.-J. Schulz, J. Phys.: Condens. Matter **4** (1992) 8253.
3. P. Peka, H. R. Selber, H.-J. Schulz, R. Schwarz and K. W. Benz, Solid State Commun. **98** (1996) 677.
4. P. Peka, M. U. Lehr, H.-J. Schulz, U. Pohl, J. Kreissl and K. Irmscher, Phys. Rev. B **53**, (1996) 1907.
5. J. Schneider, B. Dischler and A. Räuber, Solid State Commun. **5** (1967) 603.
6. J. Kreissl, K. Irmscher, P. Peka, M. U. Lehr, H.-J. Schulz and U. W. Pohl, Phys. Rev. B **53** (1996) 1917.

7. P. Christmann, B. M. Meyer, J. Kreissl, R. Schwarz and K. W. Benz, Phys. Rev. B **53** (1996) 3634.
8. P. Christmann, J. Kreissl, D. M. Hofmann, B. K. Meyer, R. Schwarz and K. W. Benz, J. Crystal Growth **161** (1996) 259.
9. A. Harrison, *Electronic Structure and the Properties of Solids* (Freeman, N.Y., 1980).
10. F. S. Ham, Phys. Rev. **138** (1965) A1727.
11. I. B. Bersuker and V. Z. Polinger, *Vibronic Interactions in Molecules and Crystals*, Springer Series in Chemical Physics, vol. **49**, Berlin 1989, Ch. 3.
12. M. Caner and R. Englman, J. Chem. Phys. **44** (1966) 4054.
13. R. E. Trees, Phys. Rev. **85** (1952) 382.
14. W. M. Theis, K. K. Bajaj, C. W. Litton and W. G. Spitzer, Appl. Phys. Lett. **41** (1982) 70.
15. A. J. Mayur, M. Dean Sciacca, I. Miotkowski, G. C. La Rocca, A. K. Ramdas and S. Rodriguez, Solid State Commun. **91** (1994) 785.